9-30-2022

Hydrogel and Graphene Embedded Piezoresistive Microcantilever Sensor for Solvent and Gas Flow Detection

Dipannita Ghosh
The University of Texas Rio Grande Valley

Md. Ashiqur Rahman
The University of Texas Rio Grande Valley

Ali Ashraf
The University of Texas Rio Grande Valley

Nazmul Islam
The University of Texas Rio Grande Valley, nazmul.islam@utrgv.edu

Recommended Citation

Ghosh, D, Rahman, MA, Ashraf, A, & Islam, N. "Hydrogel and Graphene Embedded Piezoresistive Microcantilever Sensor for Solvent and Gas Flow Detection." Proceedings of the ASME 2022 17th International Manufacturing Science and Engineering Conference. Volume 1: Additive Manufacturing; Biomanufacturing; Life Cycle Engineering; Manufacturing Equipment and Automation; Nano/Micro/Meso Manufacturing. West Lafayette, Indiana, USA. June 27–July 1, 2022. V001T07A012. ASME. https://doi.org/10.1115/MSEC2022-85544

Proceedings of the ASME 2022
Manufacturing Science and Engineering Conference
MSEC2022
June 27- July 1, 2022, Purdue University, Indiana, USA

MSEC2022-85544

HYDROGEL AND GRAPHENE EMBEDDED PIEZORESISTIVE MICROCANTILEVER SENSOR FOR SOLVENT AND GAS FLOW DETECTION

Dipannita Ghosh*,[1], Md. Ashiqur Rahman*,[1], Ali Ashraf[1], Nazmul Islam[1]
*Equal contribution
[1]The University of Texas Rio Grande Valley, TX, USA-78539.

ABSTRACT

Piezoresistive microcantilever sensor is widely used in sensing applications including liquid and gas flow detection. Microcantilevers can function as an embedded system if they are coated with polymers or nanomaterials to improve sensing performance. In this paper, we investigated the performance of piezoresistive microcantilevers (PMC) with and without additional coating. We studied the sensitivity of the PMC sensor after coating it with a three-dimensional porous hydrogel and piezoresistive graphene oxide layer. Hydrogel-embedded piezoresistive microcantilever (EPM) showed better results than PMC during solvent sensing application. The resistance change for hydrogel embedded PMC was higher compared to bare PMC by 430% (3.2% to 17%) while detecting isopropyl alcohol (IPA), by approximately 1.5 orders of magnitude (0.19% to 5.7%) while detecting the presence of deionized water. Graphene Oxide coated PMC showed a wider detection range of 30 milliliter/min and 24% better sensitivity than bare PMC during the gas detection experiment. Additionally, we compared the experiment result with COMSOL simulation to develop a model for our embedded PMC sensing. Simulation shows significantly higher deflection of the EPM compared to the bare PMC (66.67% higher while detecting IPA, consistent with the trend observed during the experiment). The facile drop casting-based embedded microcantilever fabrication technique can lead to improved performance in different sensing applications. Our future work will focus on detecting biomolecules by using our constructed embedded systems.

1. INTRODUCTION

The expected high sensitivity of microcantilever-based chemical and biochemical sensing devices has sparked interest in recent years [1-5]. The microcantilever is very sensitive to surface processes because of its enormous surface area to volume ratio [6]. The cantilever itself acts as a transducer, therefore the target substance is detected in alternating or direct current (AC or DC) based microbalance method where a change in the cantilever mass is correlated with electrical signal output. The change in cantilever mass can cause a change in the cantilever's resonant frequency (AC detection) [7]. On the other hand, in DC mode, as the target substance attaches to the surface, the surface tension changes, causing a cantilever bending as the surface expands or contracts to balance the surface energy shift. In our proposed method, we have employed the DC method because of its simplicity.

The bending of the microcantilever is proportional to the surface coverage of the absorbed molecule[8-10]. A differential surface tension is created between the two sides when the adsorption of molecules on the surface of thin material is limited largely to one side, for example, by rendering the opposing surface inert[11]. The material deforms due to the difference in surface stress. The Shuttleworth equation may be used to link surface stress, σ, and surface free energy, γ:

$$\sigma = \gamma + \frac{d\gamma}{d\varepsilon} \quad (1)$$

Here, $d\varepsilon$ refers to the ratio of the change in surface area to total area. For liquid, the differential part becomes zero. Stoney's equation can be used to find the relation between difference in surface stress Δσ and the difference of the deflection between untreated surface and chemically modified surface, Δh:

$$\Delta h = \frac{3(1-v)L^2}{Et^2}(\Delta\sigma 1 - \Delta\sigma 2) \quad (2)$$

In the above equation, v stands for the Poisson ratio of the material, E is for Young's(elastic) modulus of the cantilever material, and L is for length and t is the length of the cantilever.

In Piezoresistive microcantilever (PMC) sensor, chemical, physical, or other reactions with the sensor material causes the cantilever to bend when exposed to analyte [12], which causes the sensor electronics to measure this bending as a simple resistance change. The key benefits of the microcantilever method are its sensitivity, which is based on the capacity to detect cantilever motion with sub-nanometer accuracy, and ease of manufacturing a multi-element sensor array [13]. Due to established fabrication methods and outstanding material characteristics, piezoresistive cantilever sensors are commonly built on silicon-on-insulator (SOI) substrates [14].

The embedded piezoresistive microcantilever (EPM) sensor is a modern version of this method [15]. The piezoresistive microcantilever is entirely or partially immersed in the sensing material. The cantilevers themselves may only be a few tens of microns in size, resulting in a very rigid and robust sensor element that is immune to movement or external disturbance [16]. Analyte molecules may adsorb on the surface, physically partition into, covalently link to, or otherwise insert themselves into the sensing material layer, depending on the sensing material. The action causes a higher volumetric or vertical change in the embedded microcantilever, thereby causing larger deflection compared to PMC. Strains as small as a few Angstroms can be measured using EPM sensor. EPM sensors have been employed in a range of sensing applications, including the detection of animal presence, hydrogen fluoride gas [12], organophosphate gases [17], volatile organic compounds (VOCs), carbon monoxide gas [15], hydrogen cyanide gas [18], and others. Microcantilever flow sensors have also gained popularity in recent years due to their low power consumption, low manufacturing costs, compact size, and great sensitivity [19]. According to a theoretical model developed by Wenzel et al., a sensing material with a high Young's modulus gives great sensitivity [20, 21]. Because Young's modulus of graphene oxide is so large [22], great sensitivity for graphene-based microcantilever sensors in the static mode is predicted.

In this paper, we have explored the performance of a silicon-based piezoresistive microcantilever with an Agarose hydrogel and graphene oxide coating-based embedding system for solvent and gas flow sensing. According to our findings, the piezoresistive microcantilever's sensing ability is greatly enhanced after embedding. We validated the experimental result with COMSOL Multiphysics software. This gives us the platform to further extend our experimental work in stress sensing and various biological molecules detection.

2. MATERIALS AND METHODS

2.1 Experimental setup

Cantimer, Inc., Menlo Park, CA, designed the piezoresistive microcantilevers used in the experiments [23]. The microcantilevers, which are individually encased in a silicon die chip, are around 200 micrometers long and 40 micrometers broad. Each cantilever on each chip extends into a small circular space to confine the sensing material and protect it during sensor assembly. Each die also has an inbuilt thermistor for temperature adjustment for the situations where temperature information is required. Figure 1(a) shows an image of a single cantilever tip under the microscope. Before embedding the cantilever, the resistance is around 2.3 kΩ in normal conditions. The room temperature while experimenting is approximately 21˚C.

For a controlled experiment, a 3D printed microcantilever chamber is built. The piezoresistive microcantilever is inserted into the 3D-printed chamber, and the cantilever pin is attached to a B&K Precision Multimeter. The multimeter is interfaced using 2831E and 5491B Multimeter Software. Figure 1(c) shows the entire liquid sensing experimental setup. We have used the same experimental setup for gas flow detection as we have used for liquid sensing. In addition, the 3D printed chamber's opening is now connected to an air cylinder. For airflow control, a trace gas mixer is used in this experiment. The full gas flow sensing experimental setup is depicted in Figure 1(d).

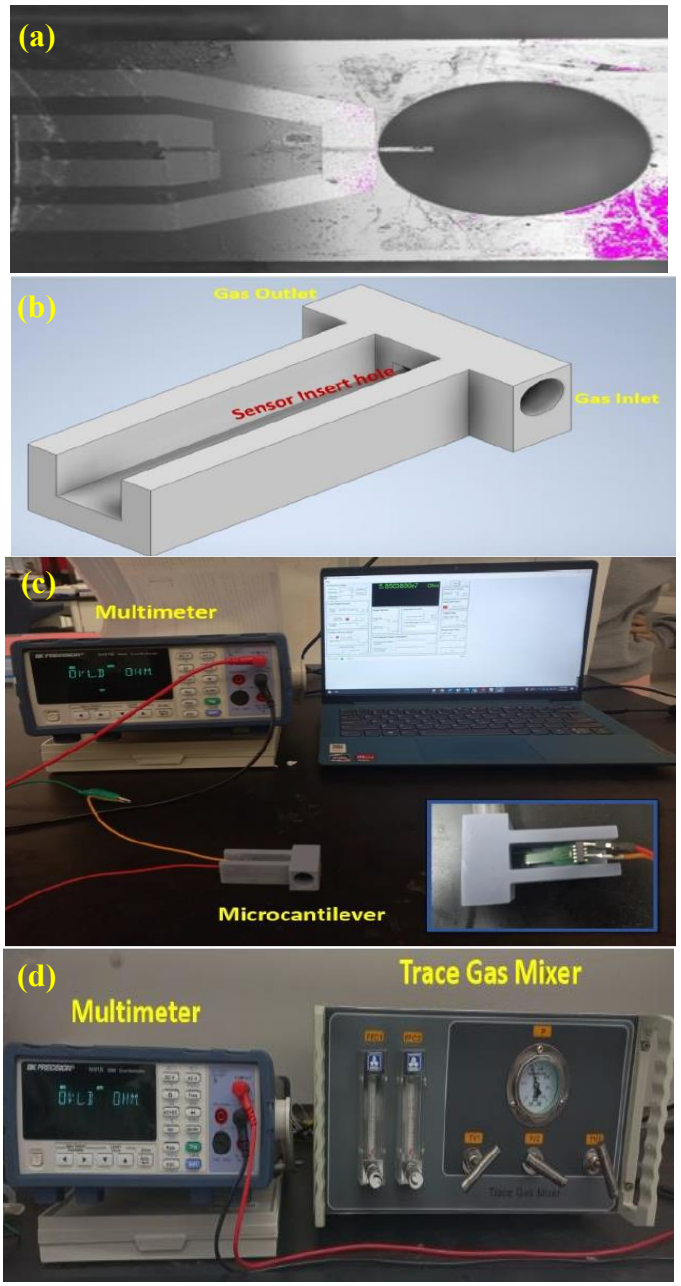

Figure 1: Experimental setup for liquid and gas sensing with piezoresistive microcantilever sensor (a) microcantilever tip under a microscope, (b) Computer-Aided Design of 3D microcantilever chamber, (c) experimental setup for liquid sensing (microcantilever connection at inset), (d) experimental setup for gas flow rate measurement.

For embedding the hydrogel, we have employed A2576 (Sigma Aldrich) Agarose for hydrogel embedding, which has a gelling point of 20˚C and a melting point of 62˚C. We combined 2.9 gm hydrogel with 9.67 gm Phosphate-Buffered Saline (PBS) and heated it for 15 minutes at 60˚C. After that, the solution is allowed to cool for 30 minutes. However, as the hydrogel grows stickier, pouring it into the micro pipet becomes more difficult. So, we warmed the solution again to make it less viscous before using it in the micropipette. The drop-casting method is schematically shown in Fig. 2.

Graphene oxide embedded microcantilever is used for the measurement of gas flow rate. We have mixed 0.2 gm graphene oxide with 50ml PBS(1x) for the solution. Then a micro pipet is then used to embed a 0.2 microliter solution on the tip of the microcantilever.

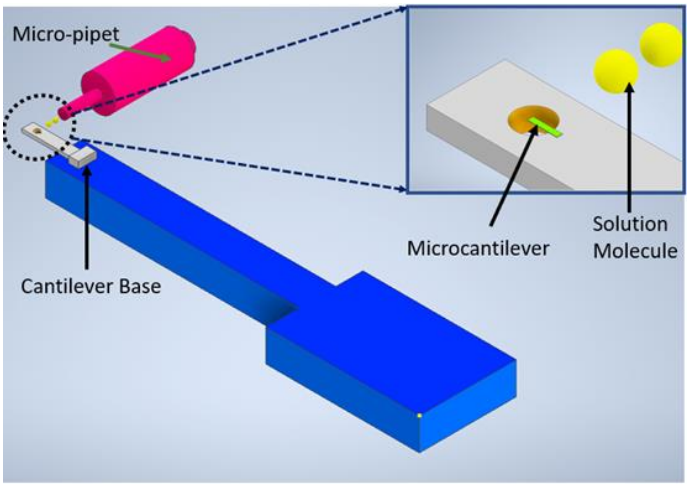

Figure 2: Schematic showing drop-casting method to coat and test microcantilever sensors.

We have used COMSOL Multiphysics software to validate our experimental result. Piezo resistivity, Domain currents Multiphysics module has been used for the simulation purpose. N-silicon (polycrystalline, weakly doped) is the material employed in the piezoresistive layer. The substrate of the microcantilever is made of silicon (Si- Polycrystalline Silicon). For the hydrogel (Agarose coating), 2-micrometer layers have been added on the tip of the microcantilever in the 'geometry' model. Young Modulus, Poison's ratio, and density have been inserted in the material section. We have used Physics controlled mesh (fine elements) for computing the simulation.

2.2 Experimental Procedure

We initially tested 2 microliter volumes of isopropyl alcohol (IPA), Deionized (DI water, and phosphate-buffered saline (PBS) (1x strength) on the piezoresistive microcantilever tip, recording the resistance change for roughly 800 seconds. Then we have repeated the same experiment with hydrogel embedded microcantilever. For the gas flow meter experiment, we first circulated air at various flow rates on the microcantilever tip and measured resistance as a function of flow rate. Further, the experiment is repeated with a microcantilever tip coated with graphene oxide.

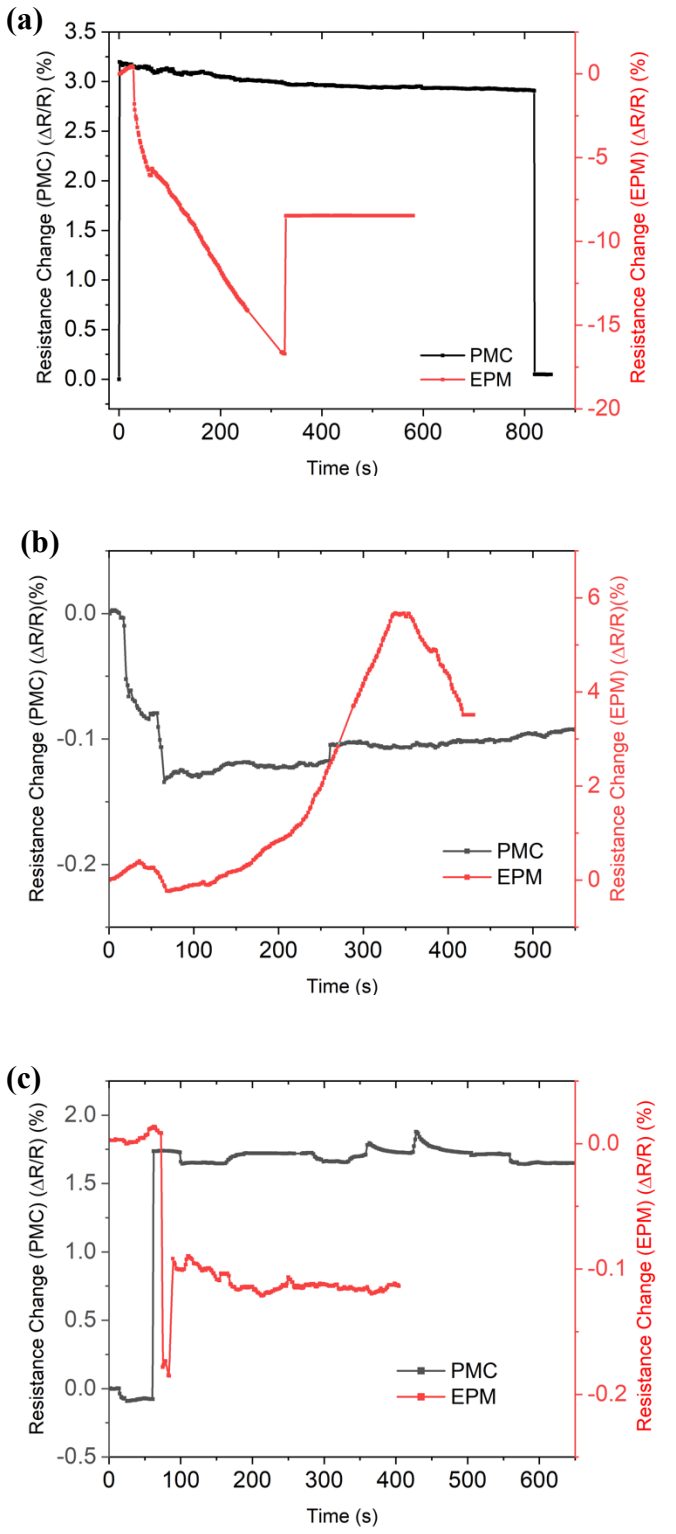

Figure 3: Resistance Versus Time during (a) IPA (b) DI and (c) PBS exposure for both PMC and EPM.

3. RESULTS AND DISCUSSION

The amount of bending determines the resistance of the piezoresistive cantilever. The bending changes the displacement of the free end of the PMC due to changes in weight and intermolecular interactions, which in turn is converted to a resistance change. The resistance change during exposure to three solutions, namely IPA, DI water, and PBS was determined for piezoresistive microcantilever with or without a hydrogel coating (Fig. 3).

Because IPA is a volatile liquid, it quickly evaporated after being dropped on the microcantilever's tip. As a result, resistance increased to a peak, then began to decrease, and the microcantilever gradually returned to its original position (Fig. 3a). When comparing hydrogel embedded EPM results to PMC alone, the percentage change of resistance rose by almost 430 percent (3.2 % to 17 %). A stable value of resistance was achieved at approximately 320s because of dehydration of the hydrogel during IPA evaporation (Fig. 3a). The resistance changed rapidly for 2µl of DI water drop casting from a fixed height (0.5 cm) due to the surface tension of the water droplet. It attained a stable value after around 600 seconds, suggesting the presence of water particles on the tip (Fig. 3b). Because agarose hydrogel is a typical strongly hydrophilic material, DI water with hydrogel embedded EPM was tested. The highest resistance change of DI water in the presence of hydrogel is 5.7% (Fig. 3b). This indicates an increase in the order of 1.5 for hydrogel embedded EPM compared to only PMC. Agarose hydrogel being neutral in nature, shows more ionization at low pH. An ionized hydrogel has more charges in it; thus it creates electrostatic repulsion between polymer chains. The more ionized a hydrogel is, the more charges it has, creating electrostatic repulsion between polymer chains [24]. The network becomes more hydrophilic, and the degree of swelling increases, resulting in a larger deflection of the EPM. As IPA has low pH (5.3 to 5.4) and DI water is neutral (PH 7.00), the agarose hydrogel is a good choice for detecting these solvents. As can be seen in plot 3(a-c), the hydrogel-based EPM shows larger deflection for IPA (~17%) as compared to DI (~6%) due to enhanced electrostatic interaction at low pH IPA.

Resistance to PBS peaks shortly after a drop of 2µl on the tip of the microcantilever. However, in this case, the deflection and response of PMC are better than EPM (1.7% vs 0.17%). We think the interaction between charged polymer chains of agarose hydrogel and ions in phosphate buffer saline leads to competing effects of downward deflection due to weight and upward deflection due to electrostatic forces. More investigation is required to capture this phenomenon. We hope to address this in future publications.

Graphene Oxide (GO)-PBS solution was applied to the microtip to form a coating after evaporation of the liquid. After PMC contact with GO-PBS solution, the resistance change reaches a stable value of 0.06% at around 1600 sec (0.2 percent GO), indicating a Graphene Oxide coating has been formed on the PMC after IPA droplet evaporation (Fig. 4a). This graphene oxide-coated tip was used to investigate airflow for a very small change in flow rate regulated by a needle valve. Results show that the micro-cantilever with a small amount of Graphene Oxide coating has a longer range (i.e., resistance change is distinguishable after 130 ml/min) than the micro-cantilever that does not have GO coating (Fig. 4b &c).

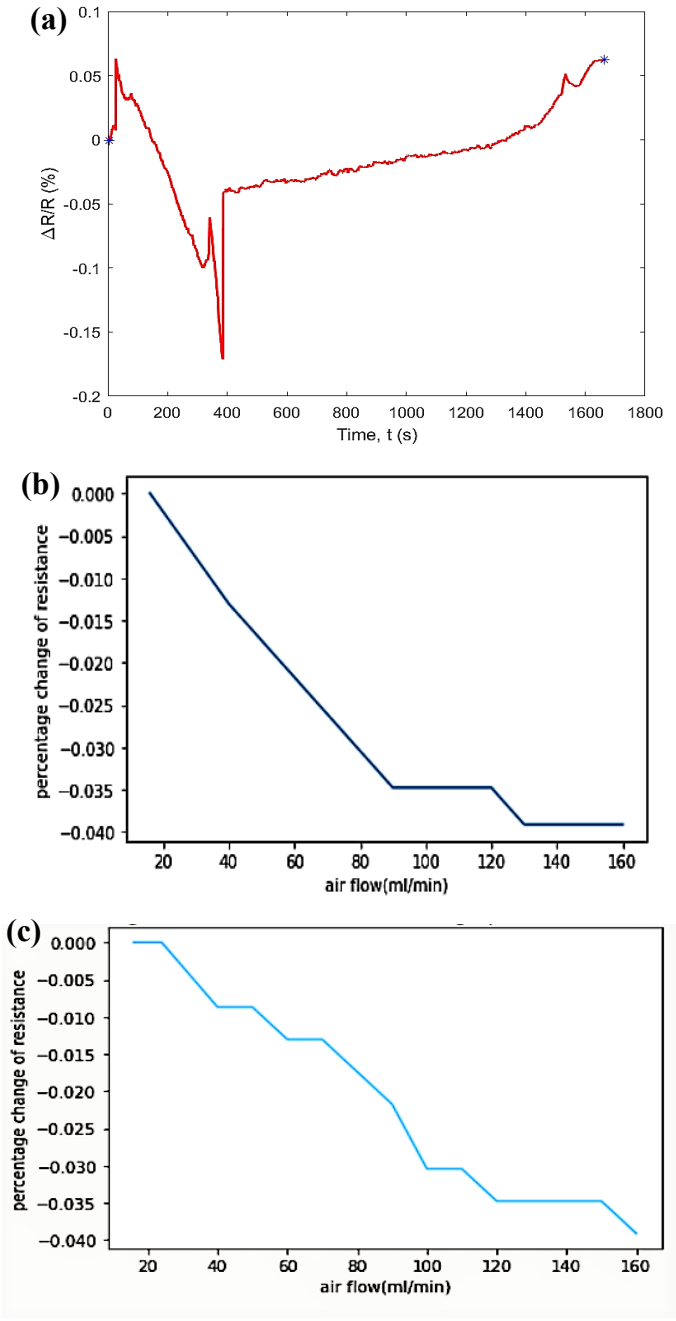

Figure 4: Resistance Change (%) (a) during GO coating (b) vs. airflow for PMC (c) vs. airflow for EPM with GO coating.

The resistance for airflow was decreasing proportionally to the increased airflow up to 90 ml/min, then became constant up to 120ml, and a similar trend was found afterward (Fig. 4b). But, for the airflow with graphene-coated PMC, the slope changed frequently and then became constant (Fig. 4c). We think that the nonlinear response of GO embedded EPM may be due to poor

adhesion between the cantilever and graphene oxide. Since the coating process depended on physical attraction rather than chemical bonding, the noisy response can be correlated to this aspect of fabrication. In the future, we shall try to try to attach GO to silicon microcantilever through chemical bonding. The slope for GO-coated EPM was ~24% higher between 60-100 mL/min compared to PMC without coating (0.000425 vs 0.000325), indicating better sensitivity for GO-coated EPM.

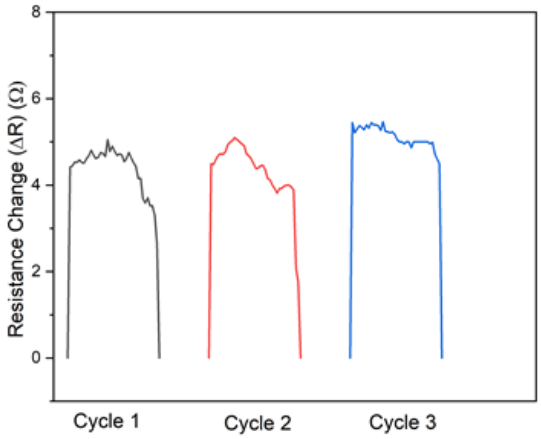

Figure 5: Repeatability test of PMC with IPA.

To test the cyclic performance of the PMC, we drop casted IPA on it and waited for the droplet to evaporate 3 different times. The PMC showed repeatable performance and went back to its original state after IPA evaporation (Figure 5).

COMSOL Multiphysics software is used to validate our experimental result. At first, the simulation is done using a PMC without using embedded hydrogel for the solvent IPA, DI water & PBS. Then the performance is compared with the hydrogel embedded one for the same solvents. In each case, hydrogel embedded microcantilever outperformed the microcantilever without embedding. IPA has shown the best result, where the highest tip displacement has been increased by 66.67% after embedding the piezoresistive microcantilever (Fig. 6).

For DI water, maximum tip displacement for uncoated piezoresistive microcantilever is 0.09 micrometer and after embedding, maximum tip displacement increased by 0.03 micrometer with an increase of 55.56% (Fig. 7).

And for PBS solution, the maximum tip displacement increased by 0.04 micrometer after embedding the microcantilever with an increase of 33.33% (Fig. 8).

4. Conclusion

In conclusion, we used both PMC and hydrogel/GO coated EPM to detect solvents and gases. When it comes to solvent sensing, EPM performs better than PMC (400% to 1.5 order of magnitude better performance). In addition, a facile drop casting-based embedded microcantilever fabrication technique incorporating GO nanomaterial extends the gas detection range and provides better sensitivity (~24% higher). A COMSOL simulation yields comparable results to the experiments for solvents such as IPA, DI water, and PBS. Our facile embedding technique has the potential to enable sensitive detection of biomolecules using nanomaterial/hydrogel coated piezoresistive microcantilevers.

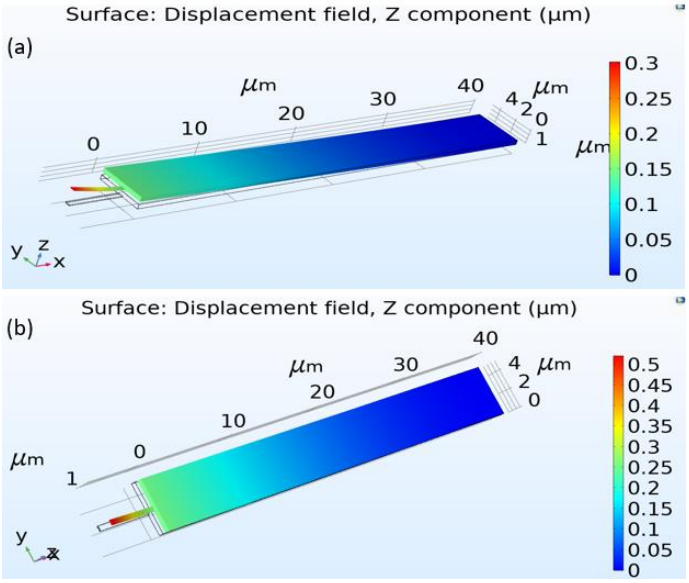

Figure 6: COMSOL simulation of microtip displacement for IPA a) without Hydrogel b) with Hydrogel.

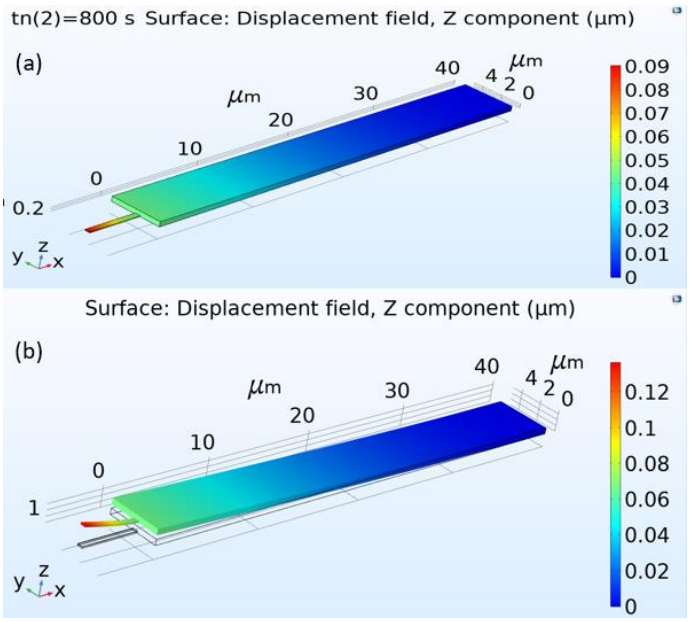

Figure 7: COMSOL simulation of microtip displacement for DI Water a) without Hydrogel b) with Hydrogel.

ACKNOWLEDGEMENTS

We kindly acknowledge the instrumentation support and suggestions provided by Mr. Omar Castelan and Mr. Omar from the Department of Electrical Engineering at The University of Texas Rio Grande Valley. We also thank COMSOL for providing software support.

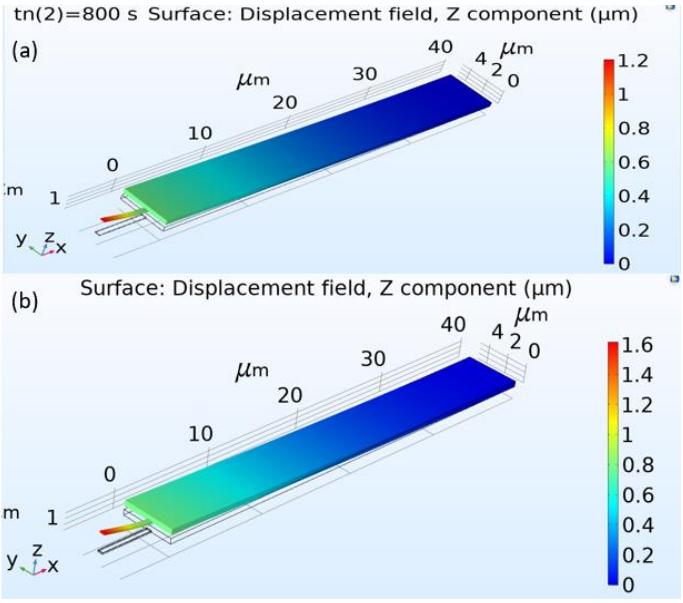

Figure 8: COMSOL simulation of microtip displacement for PBS a) without Hydrogel b) with Hydrogel.

REFERENCES

[1] Goeders, K. M., Colton, J. S., and Bottomley, L. A., 2008, "Microcantilevers: sensing chemical interactions via mechanical motion," Chemical reviews, 108(2), pp. 522-542.

[2] Boisen, A., Dohn, S., Keller, S. S., Schmid, S., and Tenje, M., 2011, "Cantilever-like micromechanical sensors," Reports on Progress in Physics, 74(3), p. 036101.

[3] Li, X., and Lee, D.-W., 2011, "Integrated microcantilevers for high-resolution sensing and probing," Measurement Science and Technology, 23(2), p. 022001.

[4] Sepaniak, M., Datskos, P., Lavrik, N., and Tipple, C., 2002, "Peer reviewed: Microcantilever transducers: A new approach in sensor technology," ACS Publications.

[5] Zhu, Q., 2011, "Microcantilever sensors in biological and chemical detections," Sensors & transducers, 125(2), p. 1.

[6] Dufour, I., Lemaire, E., Caillard, B., Debéda, H., Lucat, C., Heinrich, S. M., Josse, F., and Brand, O., 2014, "Effect of hydrodynamic force on microcantilever vibrations: Applications to liquid-phase chemical sensing," Sensors and Actuators B: Chemical, 192, pp. 664-672.

[7] Tamayo, J., Humphris, A., Malloy, A., and Miles, M., 2001, "Chemical sensors and biosensors in liquid environment based on microcantilevers with amplified quality factor," Ultramicroscopy, 86(1-2), pp. 167-173.

[8] Craighead, H., 2007, "Measuring more than mass," Nature nanotechnology, 2(1), pp. 18-19.

[9] Naik, A. K., Hanay, M., Hiebert, W., Feng, X., and Roukes, M. L., 2009, "Towards single-molecule nanomechanical mass spectrometry," Nature nanotechnology, 4(7), pp. 445-450.

[10] Raiteri, R., Nelles, G., Butt, H.-J., Knoll, W., and Skládal, P., 1999, "Sensing of biological substances based on the bending of microfabricated cantilevers," Sensors and Actuators B-Chemical, 61(1-3), pp. 213-217.

[11] Senesac, L. R., Yi, D., Greve, A., Hales, J. H., Davis, Z. J., Nicholson, D. M., Boisen, A., and Thundat, T., 2009, "Micro-differential thermal analysis detection of adsorbed explosive molecules using microfabricated bridges," Review of Scientific Instruments, 80(3), p. 035102.

[12] Porter, T. L., Vail, T., Wooley, A., and Venedam, R. J., 2010, "Detection of chlorine gas using embedded piezoresistive microcantilever sensors," Sensors and Materials, 22(3), pp. 101-107.

[13] Ji, H.-F., Hansen, K., Hu, Z., and Thundat, T., 2001, "Detection of pH variation using modified microcantilever sensors," Sensors and Actuators B: Chemical, 72(3), pp. 233-238.

[14] Pandya, H., Kim, H. T., Roy, R., and Desai, J. P., 2014, "MEMS based low cost piezoresistive microcantilever force sensor and sensor module," Materials science in semiconductor processing, 19, pp. 163-173.

[15] Kooser, A., Gunter, R. L., Delinger, W. D., Porter, T. L., and Eastman, M. P., 2004, "Gas sensing using embedded piezoresistive microcantilever sensors," Sensors and Actuators B: Chemical, 99(2-3), pp. 474-479.

[16] Porter, T. L., Eastman, M. P., Macomber, C., Delinger, W. G., and Zhine, R., 2003, "An embedded polymer piezoresistive microcantilever sensor," Ultramicroscopy, 97(1-4), pp. 365-369.

[17] Porter, T. L., Vail, T., Propper, C. R., and Islam, N., 2010, "Bio-composite materials for the detection of estrogen in water using piezoresistive microcantilever sensors," MRS Online Proceedings Library, 1253(1), pp. 10-15.

[18] Porter, T. L., Vail, T. L., Eastman, M. P., Stewart, R., Reed, J., Venedam, R., and Delinger, W., 2007, "A solid-state sensor platform for the detection of hydrogen cyanide gas," Sensors and Actuators B: Chemical, 123(1), pp. 313-317.

[19] Bleckmann, H., Klein, A., and Meyer, G., 2012, "Nature as a model for technical sensors," Frontiers in Sensing, pp. 3-18.

[20] Heinrich, S. M., Wenzel, M. J., Josse, F., and Dufour, I., 2009, "An analytical model for transient deformation of viscoelastically coated beams: Applications to static-mode microcantilever chemical sensors," Journal of Applied Physics, 105(12), p. 124903.

[21] Wenzel, M. J., Josse, F., Heinrich, S. M., Yaz, E., and Datskos, P., 2008, "Sorption-induced static bending of microcantilevers coated with viscoelastic material," Journal of Applied Physics, 103(6), p. 064913.

[22] Papageorgiou, D. G., Kinloch, I. A., and Young, R. J., 2017, "Mechanical properties of graphene and graphene-based nanocomposites," Progress in Materials Science, 90, pp. 75-127.

[23] Gunter, R., Delinger, W., Porter, T., Stewart, R., and Reed, J., 2005, "Hydration level monitoring using embedded piezoresistive microcantilever sensors," Medical engineering & physics, 27(3), pp. 215-220.

[24] Deligkaris, K., Tadele, T. S., Olthuis, W., and van den Berg, A., 2010, "Hydrogel-based devices for biomedical applications," Sensors and Actuators B: Chemical, 147(2), pp. 765-774.